PERIODICA POLYTECHNICA SER. EL. ENG. VOL. 38, NO. 4, PP. 361-372 (1994)

NUMERICAL SIMULATIONS OF MAGNETIC BRUSH FORMATION PHENOMENA

Zoltán CSAHÓK*, Hajime IGARASHI***, Toshihsa HONMA***
and Tamás VICSEK**

* Department of Atomic Physics
Eötvös University Budapest
1088 Budapest, Hungary

** Institute for Technical Physics
P. O. Box 76, 1325 Budapest, Hungary

*** Department of Electrical Engineering
Hokkaido University Sapporo
North 13. West 8., Japan

Received: Nov. 1, 1994

Abstract

We have developed models capable of describing magnetic brush formation phenomena. In particular, we investigate the effects of physical parameters (applied magnetic field, etc.) on the correlations and the structure. Three models are presented, which point out different aspects of the brush growth process.

Keywords: magnetic brush, fractal, numerical simulation.

1. Introduction

The formation of magnetic brushes is a common phenomenon in electrophotography [1]. A magnetic brush is an aggregate of small (about 10 microns in diameter) paramagnetic particles forming a bristle in an applied magnetic field. In electrophotography, the toner particles form magnetic brushes on the surface of a magnetic roller which transfers them from a hopper area to the development zone. Although magnetic brush formation is a well-known phenomenon, the physical characteristics remain still unclear. For this reason, the effects of the magnetic brush have been neglected in computer simulations of electrophotographic developments [2, 3] in spite of their importance.

2. The Models

The physical system we simulate by our models consists of toner beads sedimenting in uniform magnetic ($\mathbf{B}_{ext}$) and gravitational ($\mathbf{g}$) fields perpen-

dicular to the baseline (*Fig. 1*). The gravity makes the beads to sediment and the external magnetic force causes the brushes to be formed. Based on the assumption that the third dimension has no specific role in the chain formation in our models the process is considered to be two dimensional, i.e., no movement in the y direction is allowed. These models can also have applications in studying electrorheological fluids [4] since the background processes (magnetic and electric dipole–dipole interaction) are analogous.

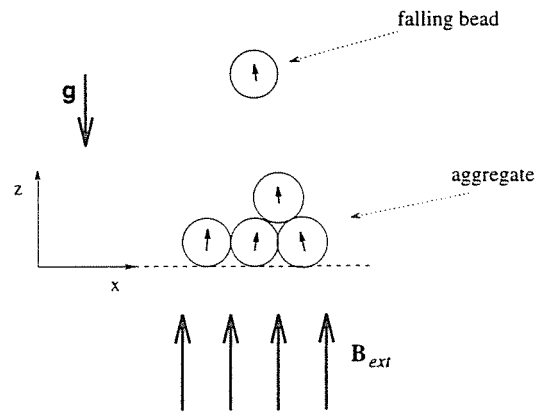

Fig. 1. The physical process: a falling bead in uniform magnetic and gravitational field. The magnetic field at the position of the falling bead is the sum of the external field and the field due to induced magnetic momenta, which are represented by the small arrows inside the beads

First we propose a very simple model (*Model A*) which tries to pick the key features of the sedimentation process. We consider aggregation of disks over a line, similarly to ballistic deposition models [5, 6]. Taking into account all physical parameters this makes the aggregation process very complicated and time consuming to simulate. For this reason we have chosen a simplified interaction between the depositing toner particle and the aggregate, which reflects nevertheless the main features of the magnetic dipole–dipole interaction. The particles at the top of the chains, forming the magnetic brush have uncompensated magnetic momenta, so they can attract the incoming particles from a longer distance than the ones within the chains whose momenta are compensated by the neighboring beads. Thus our model is the following:

i. we choose a random position along x axis and drop a particle vertically;

ii. if the falling particle gets closer to a *top* particle than a given r_a distance then it changes its path and moves to this attracting particle along a straight line;

iii. if the falling particle touches a particle within a chain, then it is attached to it irreversibly.

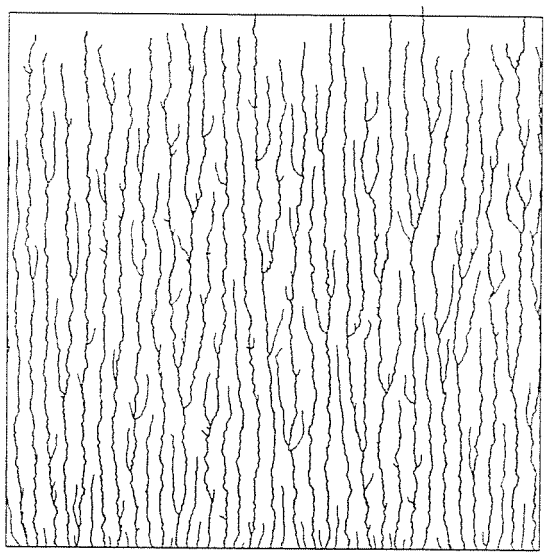

Fig. 2. Aggregate generated by Model A. (32767 particles, system size 1500 particles)

The aggregate considered to be static during the process and the deposition is performed by repeating steps above using periodic boundary conditions. The latter means that the right and the left sides of the system are connected, this is an approximation of an infinite system. The growth process yields a tree-like structure (*Fig. 2*, 32767 particles) with a characteristic distance $\lambda = 2r_a$. *Fig. 3* shows the horizontal correlation function $c(r)$ for this aggregate, which is defined as follows. Let us first introduce the function which shows if two beads are in distance r along the x axis and have the same z coordinate:

$$\eta_{ij}(r) = \begin{cases} 1, & \text{if } r < x_{ij} < r + \Delta r \text{ and } z_{ij} < \Delta z; \\ 0, & \text{otherwise,} \end{cases}$$

where x_{ij} and z_{ij} denote the distance of the ith and the jth bead along the horizontal (x) and vertical (z) axes, respectively. Δr and Δz are suitably chosen constants of the order of the bead size. Using the η_{ij} function the

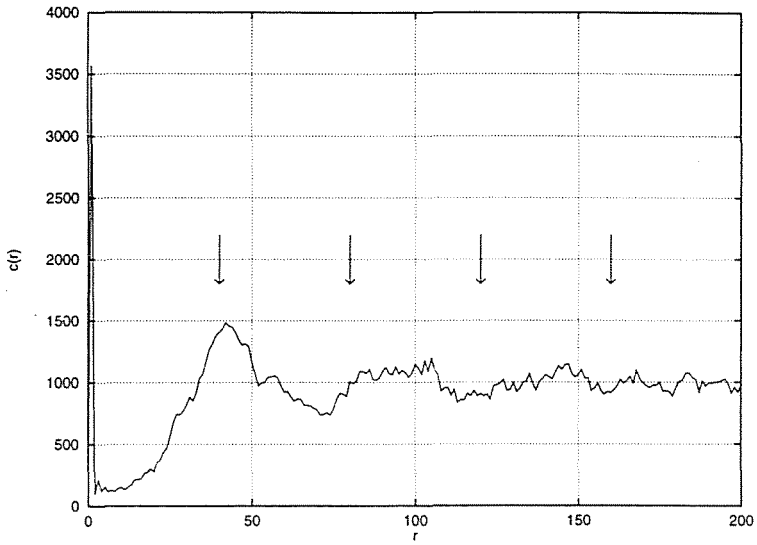

Fig. 3. Correlation function for aggregate on *Fig. 2*

horizontal correlation function is defined as its sum over all possible disk pairs

$$c(r) = \frac{1}{2}\sum_{i\neq j}^{N} \eta_{ij}(r),$$

where N is the number of beads in the aggregate. The summation yields an average over the z direction, for this reason this function is called horizontal correlation function. The arrows in the figure show the expected correlation maxima for $\lambda = 40$, rather good coincidence can be seen, the first maximum of $c(r)$ is at $r = 40$, the next maxima are not that pronounced but still close to their theoretical values ($r = 80, 120, 160$). We showed that the $c(r)$ function is a good mean for characterizing periodicity of the magnetic brush.

As a next step we simulated the deposition by taking into account the magnetic field of the entire aggregate, which is a more appropriate model for the real physical process.

Model B is as follows: we take a toner bead high above the aggregate, and let it fall. There will be gravitational and magnetic forces acting on it. Gravity is a constant field, and magnetic forces in the dipole approximation are calculated from $-\frac{1}{2}\nabla(\mathbf{mB})$, the negative gradient of the magnetic potential energy of the bead. $\mathbf{m}$ is the induced magnetic momentum of the bead, and $\mathbf{B}$ is the field at the position of the bead which has contributions

both from the constant background field $\mathbf{B}_{ext}$ and the field due to induced magnetic momenta of the beads already in the aggregate:

$$\mathbf{B} = \mathbf{B}_{ext} + \sum_{k=1}^{N} \mathbf{B}_k, \tag{1}$$

where $\mathbf{B}_k$ is the magnetic field induced by the kth bead's momentum. Here we suppose that characteristic length for changes in $\mathbf{B}$ is much longer than the bead size (a). As far as $\mathbf{m}$ is proportional to $\mathbf{B}$ [7]:

$$\mathbf{m} = \frac{4\pi}{\mu_0}\frac{\mu - 1}{\mu + 2}\frac{a^3}{8}\mathbf{B}, \tag{2}$$

where μ is the relative permeability of the beads and considered to be constant, that we have to calculate is actually $-\nabla(\mathbf{B}^2)$. The analytical expression can be found for the gradient and the program uses it rather than calculating numerical gradient, which could lead to instabilities.

During the falling of the particle the magnetic momenta and the position of the rest of the aggregate are fixed, the sedimentation is considered to be adiabatic. In fact it does not hold for the magnetic field but for simplicity we neglect the effect of the falling bead on the magnetic momenta of the beads already in the aggregate. This consideration becomes more exact during the aggregation process, since there will be more beads in the aggregate so one single bead will have smaller influence on their momenta. We also consider overdamped dynamics, the force is proportional to the speed, not to the acceleration. The path of the falling bead is calculated using the Euler method

$$\mathbf{r}(t+1) = \mathbf{r}(t) + (\mathbf{F}_{magn} + m\mathbf{g})\Delta t,$$

where $\mathbf{r}(t)$ is the position of the bead at time t and Δt is a small time step.

When the falling bead touches another bead in the aggregate, it gets stuck to it, and its position will be fixed during the consequent iterations. Magnetic momenta are recalculated using an iterative algorithm, and the process is repeated again. In this model the boundary conditions are not periodic, this algorithm models the aggregation of magnetic particles coming from a gap above the surface.

For control parameter we have chosen the relative strength of the magnetic force compared to the gravity, this ratio is denoted by a dimensionless number κ. The magnitude of the magnetic force is proportional to $\mathbf{B}_{ext}^2$ and the gravitational force is the weight of the bead (mg), so that

$$\kappa \sim \frac{\mathbf{B}_{ext}^2}{mg}.$$

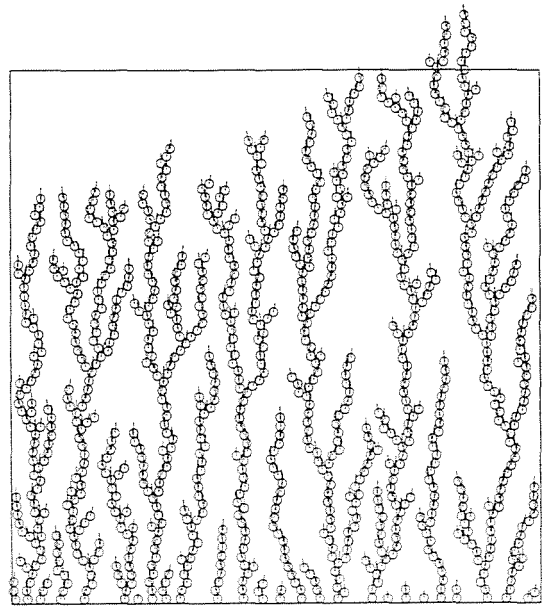

Fig. 4. Aggregate generated by Model B for $\kappa = 5$

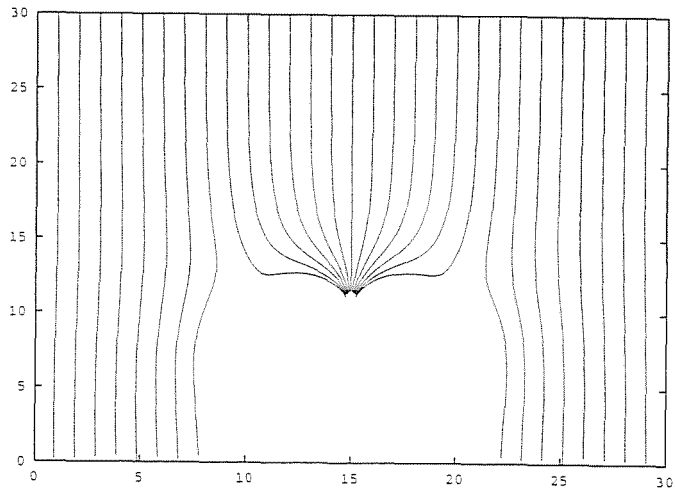

Fig. 5. Path of sedimenting particles in the field of a fixed bead at (15,15). ($\kappa = 2000$)

κ is also proportional to $\frac{\mu-1}{\mu+2}$ (see *Eq.* (2)), so all references to low magnetic field case can be thought as the limit $\mu \to 1$.

The results for the high magnetic field case ($\kappa \gg 1$, *Fig. 4*) are just the same as the ones obtained using the simple Model A. Like in Model A, there is also a well defined upper limit for the initial distance of two

stuck beads, that's a falling bead cannot reach another bead if it starts far enough along the x axis. The explanation for this feature can be given by looking at the paths of beads falling in the field of one fixed bead (*Fig. 5*). They cannot reach the fixed bead if they start further than a certain critical distance (r_c). This distance is a function of the parameter κ: for $\kappa \gg 1$ the fixed bead can attract the moving one from any distance ($r_c \to \infty$), and for $\kappa \ll 1$ the gravity dominates the movement and this critical distance vanishes ($r_c \to 0$). In Model A the role of r_c is played by the external parameter r_a.

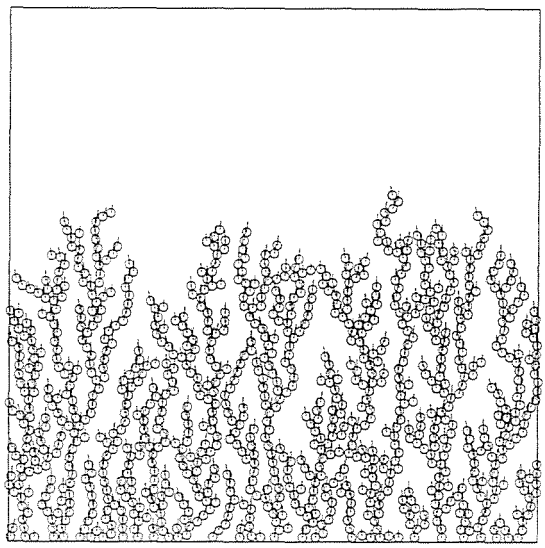

Fig. 6. Aggregate generated by Model B for $\kappa = 0$

The low magnetic field case ($\kappa \ll 1$) gives aggregates resembling off-lattice ballistic aggregates [8, 9] (*Fig. 6*). This is not surprising because in this limit the two processes are equal since only the gravity gives relevant contribution to the force acting on a bead. They fall along vertical lines and stop when they touch the aggregate. The surface of the aggregate, which is formed by the topmost beads is a fractal surface [5, 6] with roughness exponent $\alpha = 1/2$. The whole aggregate is not fractal since it has finite density of beads and an object of finite density cannot be fractal.

Even for very strong external field no straight brushes are formed in Model B as it could be expected naturally. This behavior is caused by the lack of relaxation mechanisms in the model. Our third model (*Model C*) is an enhanced version of Model B, taking into account relaxational

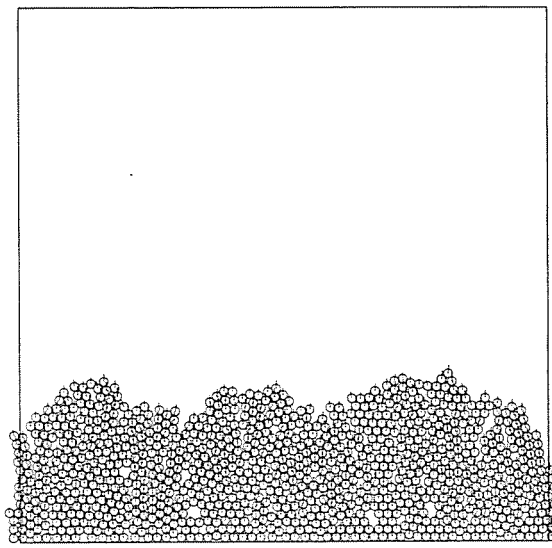

Fig. 7. Aggregate generated by Model C for $\kappa = 0$

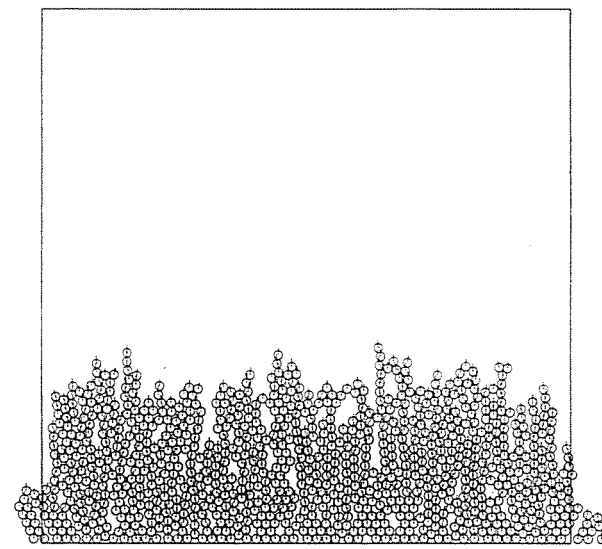

Fig. 8. Aggregate generated by Model C for $\kappa = 1$

effects which can lead to mechanical instability of the chains [10, 11]: the chains are broken if the direction of the external field is changed or they

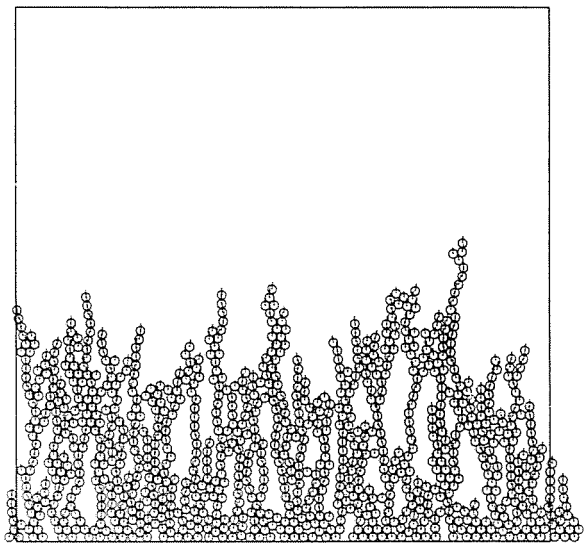

Fig. 9. Aggregate generated by Model C for $\kappa = 1.25$

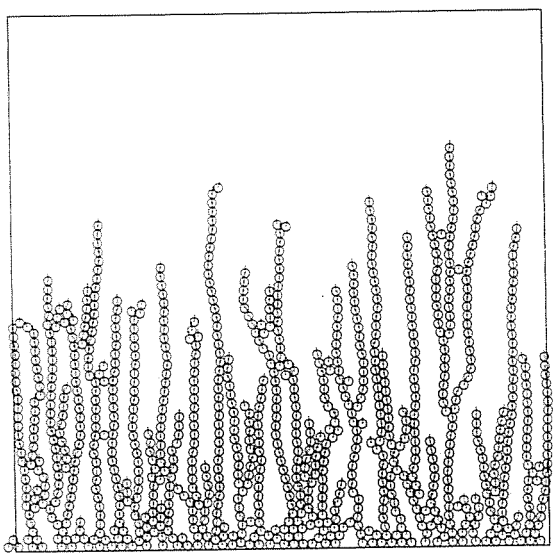

Fig. 10. Aggregate generated by Model C for $\kappa = 1.5$

become too long. Relaxation can also cause change in the structure, it allows the beads to find an energetically more optimal position and form

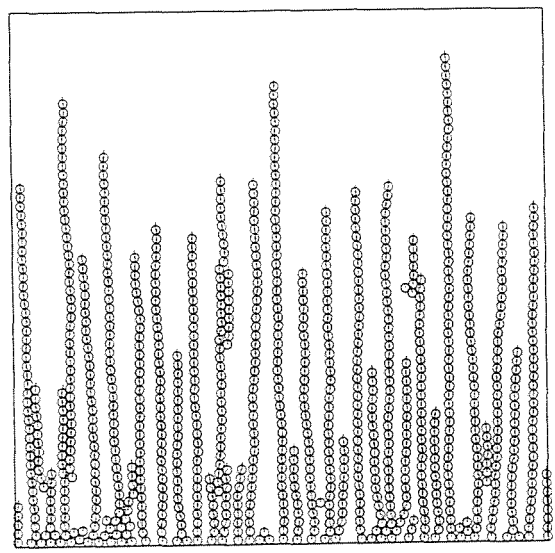

Fig. 11. Aggregate generated by Model C for $\kappa = 2$

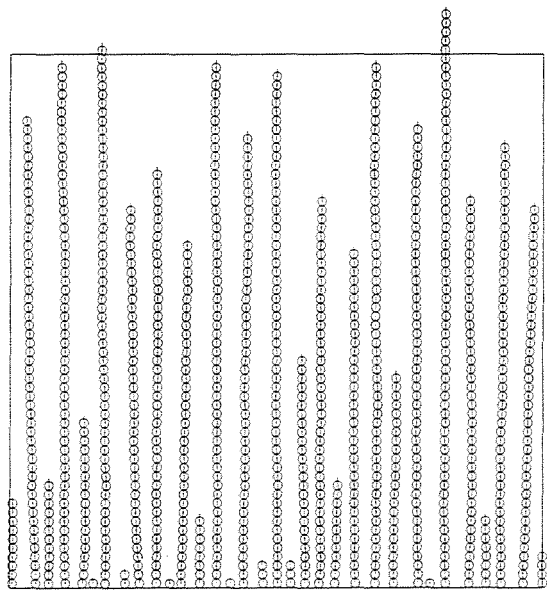

Fig. 12. Aggregate generated by Model C for $\kappa = 4$

vertical chains. The key difference between the two models is that in Model B particles are not allowed to roll on each other, but in Model C they are

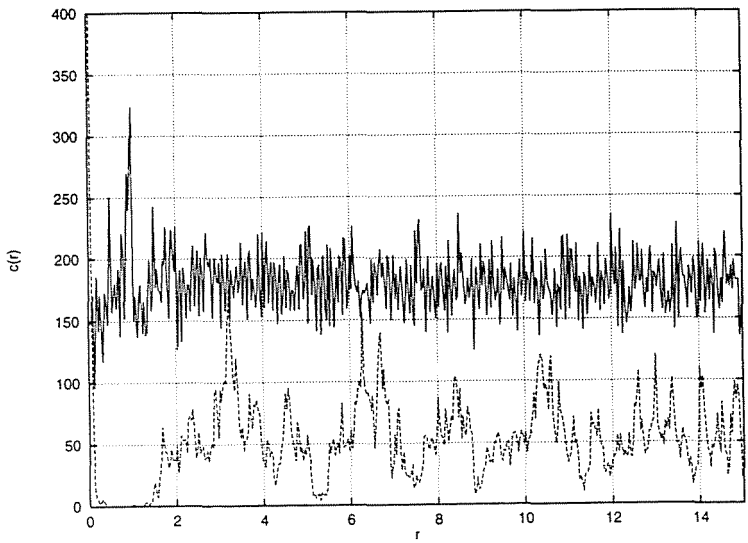

Fig. 13. Correlation function for aggregates generated by Model C for $\kappa = 0$ (solid line) and $\kappa = 4$ (dashed line)

allowed to do so. The final position of a bead is when its *local* energetical minimum is reached. This is still not a total relaxation procedure (i.e., a bead does not reach its global energy minimum position) but enough to demonstrate the difference in the aggregates. This approximation is still on the basis of adiabatical aggregation, therefore no chain breaking can occur. One should notice that when the beads are in contact we are out of the range of validity of the dipole approximation, the interaction is stronger which allows us to consider rolling of the beads on each other only.

Aggregates can be seen in *Figs. 7–12* generated by Model C for various κ values. Both aggregates consist of 1000 beads and the system size is 60 beads. Onset of periodicity, i.e., brush formation can be clearly seen as κ is increased. This feature was not present either in Model A or in Model B. *Fig. 13* shows the same type of correlation function as *Fig. 3* for Model C aggregates, the data in this figure are rather noisy because of the relatively small number of beads in the aggregate. Nevertheless, there is a well defined maximum at $r \approx 3.2$, which is a non-trivial value and expected to grow when increasing parameter κ.

Using appropriate data structure implementing Model A gives very fast code, since the algorithm is based on integer arithmetics only. The program for the Model B runs much slower than the program for the Model A. It does 1000 iterations in about 5 hours on a fast IBM RISC6000/375

workstation. This is not surprising and is related to the fact that Model B uses heavy floating point arithmetics and its algorithm is $\mathcal{O}(N^3)$. The program is vectorizable so using vector supercomputers great speed-up can be reached, and it can also allow calculation of correlation functions to higher precision and measurement of surface roughness exponents.

3. Conclusions

We have investigated three numerical models for magnetic brush formation phenomena. We can conclude that realistic chain-like patterns appear only in Model C, that is both the magnetic and the gravitational forces and relaxation have great importance on the physical process. Further work needs to be done on analyzing the stability of the aggregates against change of direction of the external magnetic field and temperature (i.e., possibility for full relaxation), applying these results in modelling the development process and for modelling magnetic fluids. Larger scale computations need to be carried out for finding fractal characterization of the surface of the brushes, which are expected to be self-affine.

We would like to thank A. Jakó for coding Model A. The present research was supported by JSAEM Grant-In-Aid for foreign researchers.

References

1. BURLAND, D. M. – SCHEIN, L. B.: Physics of Electrophotography, *Physics Today*, May 1986 pp. 46.
2. LEAN, M. H.: Simulation and Visualization of 3D Particle Cloud Electrodynamics, *IEEE Trans. Mag.* Vol. 28, p. 1271 (1992).
3. INOUE, H. – AIZAWA M. – HAYASHI, K.: Analysis of Toner Image in Developed Process for Electrophotographic Systems, *IEEE Trans. Mag.* Vol. 29, p. 1981 (1993).
4. HALSEY, T. C.: Electrorheological Fluids, *Science*, Vol. 258, p. 761 (1992).
5. FAMILY, F. – VICSEK, T. eds., Dynamics of Fractal Surfaces (World Scientific, Singapore, 1991).
6. VICSEK, T.: Fractal Growth Phenomena (World Scientific, Singapore, 1992).
7. JACKSON, J. D.: Classical Electrodynamics, (Wiley, New York).
8. MEAKIN, P. – JULLIEN, R.: Restructuring Effects in the Rain Model for Random Deposition, *J. Physique*, Vol. 48, p. 1651 (1987).
9. CSAHÓK, Z. – VICSEK, T.: Kinetic Roughening in a Model of Sedimentation of Granular Materials, *Phys. Rev.*, A, Vol. 46, p. 4577 (1992).
10. PARANJPE, R. S. – ELROD, H. G.: Stability of Chains of Permeable Spherical Beads in an Applied Magnetic Field, *J. Appl. Phys.* Vol. 60, p. 418 (1986).
11. PARANJPE, R. S. – ELROD, H. G.: A Magnetomechanical Model of the Magnetic Brush, *J. Appl. Phys.* Vol. 63, p. 2136 (1988).